Int J Legal Med (2006) 120: 233–240
DOI 10.1007/s00414-005-0023-4

ORIGINAL ARTICLE

C. Jackowski · M. Thali · E. Aghayev · K. Yen ·
M. Sonnenschein · K. Zwygart · R. Dirnhofer · P. Vock

Postmortem imaging of blood and its characteristics using MSCT and MRI

Received: 31 January 2005 / Accepted: 30 May 2005 / Published online: 19 November 2005

Abstract The rapid development of computed tomography (CT) and magnetic resonance imaging (MRI) led to the introduction and establishment in postmortem investigations. The objectives of this preliminary study were to describe the imaging appearances of the early postmortem changes of blood after cessation of the circulation, such as sedimentation, postmortem clotting, and internal livores, and to give a few first suggestions on how to differentiate them from other forensic findings. In the Virtopsy project, 95 human corpses underwent postmortem imaging by CT and MRI prior to traditional autopsy and thereof 44 cases have been investigated in this study. Postmortem alterations as well as the forensic relevant findings of the blood, such as internal or subcutaneous bleedings, are presented on the basis of their imaging appearances in multislice CT and MRI.

Keywords Virtopsy · Postmortem imaging · Blood · Internal livores · Postmortem clotting · Sedimentation

Introduction

The postmortem use of the clinically well-established tools, magnetic resonance imaging (MRI) and computed tomography (CT), for documentation of forensic findings is now being initiated [1, 13, 24, 30, 33]. Broad clinical radiological experience has been collected under vital conditions with intact circulation and metabolism following maintaining of all physiological concentrations and pressure gradients. Postmortem tissues and blood are subjected to gravity and show specific appearances, such as sedimentation processes, but blood proteins, such as fibrinogen, are still functioning. Knowledge about these phenomena is of great importance to differentiate between normal postmortem appearances and pathological findings (e.g., thrombosis, local pathological alterations in organs). Furthermore, the blood and its alterations after death often reveal forensically relevant information such as the position of the corpse after death or even direct indications to the cause of death (e.g., hemorrhage).

After cessation of the circulation, the physiology of the blood and the vascular system completely changes. The mean circulatory pressure decreases to the vital venous pressure after the blood flow has stopped, and, without further movement of the blood, all components are subjected to gravitation [23]. Under this influence, the plasma and cellular components initially sink and sediment within the vascular system of the corpse [21]. This leads to the livores of the skin and to the livores of internal organs by hemoconcentration [16, 22]. After cessation of energy-supplying processes that support the vital osmotic and colloid osmotic pressure within the vascular system, the serum and electrolytes diffuse out of the vascular lumen. In combination with hypostasis, this leads to a rise in the hematocrit up to 80% in the lower-situated and suspended regions of the corpse [17, 32]. The increased hematocrit and the decreasing temperature of the corpse cause the viscosity of the blood to increase up to a point where no passive blood flow can be induced within the small vessels by moving the corpse or even by pressure (fixed livores) [26]. Later, macromolecules in serum or intracellular ones, such as hemoglobin that are set free by the onset of hemolysis, also diffuse through the venous wall into the interstitium and intensify fixed livores [25]. The degree of hemolysis depends on the specific circumstances linked to

C. Jackowski (✉) · M. Thali · E. Aghayev ·
K. Yen · R. Dirnhofer
Institute of Forensic Medicine, University of Bern,
IRM-Buehlstrasse 20,
3012 Bern, Switzerland
e-mail: christian.jackowski@irm.unibe.ch
Tel.: +41-31-6318412
Fax: +41-31-6313833

M. Sonnenschein · P. Vock
Institute of Diagnostic Radiology, Inselspital,
University of Bern,
3010 Bern, Switzerland

K. Zwygart
Department of Clinical Research,
Magnetic Resonance Spectroscopy and Methodology,
University of Bern,
3010 Bern, Switzerland

the cause of death, which influence cell membrane stability by changing electrolyte concentrations and osmotic pressure gradients within the serum, e.g., in drowning [7, 14, 19]. Platelets and serum proteins are functionally intact for a variable time shortly after death [31]. Depending on the storage temperature, individual blood cells can be viable for up to 1 week and even longer [15]. Therefore, the cessation of circulation may induce clotting processes and thrombolysis in parallel [3–5]. The postmortem balance between the two processes is also influenced by the cause of death. High levels of catecholamines and increased plasminogen activator release by the endothelium, as often seen in cases of sudden death, intensify thrombolysis, and blood may be liquid at autopsy [27, 28]. Widespread postmortem clotting is usually seen in cases of a prolonged agonal period.

All of the procedures described occur partially in parallel and partially successively after death. Consecutively, different appearances of postmortem blood and blood-filled organs are observed, depending on the location of the blood within the corpse, the cause of death, the time after death, the position after death, the temperature within the corpse, and on other postmortem alterations such as putrefaction.

The objectives of this study are to describe the imaging appearances of the early postmortem changes of the blood after cessation of the circulation, such as sedimentation, postmortem clotting, and internal livores, and to give some initial suggestions on how to differentiate them from other forensic findings.

Materials and methods

Within the Virtopsy project, 95 human corpses underwent MRI and multislice CT (MSCT) examinations prior to autopsy up to December 2003. For the radiological examination, MSCT (four row scanner) and MRI (1.5 Tesla system) were performed. We acquired axial MSCT data with a collimation of 4×1.25 mm. The acquisition time was 10 min, and up to 1,200 axial cross-sectional images were calculated from the volumetric dataset.

MRI included, in most cases, the head, thorax, and abdomen and individually additional regions of interest such as, e.g., injuries to extremities. Coronal, sagittal, and axial images were acquired using T1-weighted fast spin echo (FSE) sequences, T2-weighted FSE sequences (with and without fat saturation), turbo inversion recovery sequences, proton density (PD) weighted spin echo sequences, and gradient echo sequences. When cardiac findings were expected, short axis, horizontal long axis, and vertical long axis images through the heart were additionally acquired. The acquisition time ranged from 1.5 to 3.5 h. Data processing and reformation of images were performed on a routine workstation. The radiological diagnoses were made by board-certified radiologists, and traditional autopsies were performed by board-certified forensic pathologists. Autopsy findings were documented by digital photography, and radiological findings from MSCT and MRI were compared to the autopsy findings in each case. For the purpose of this study of the blood, all cases that showed putrefaction/adipocere, massive destruction of the thorax, or fatal hemorrhage were excluded, leaving a total of 44 cases.

Results and discussion

Sedimentation within the heart and major vessels (Fig. 1) was visible in all investigated cases. Table 1 shows the occurrence of internal livores within lungs and liver and of postmortem clotting in the cardiac cavities and major vessels by postmortem imaging. It also lists the causes of death in each case. Sedimentation was seen in all 44 cases

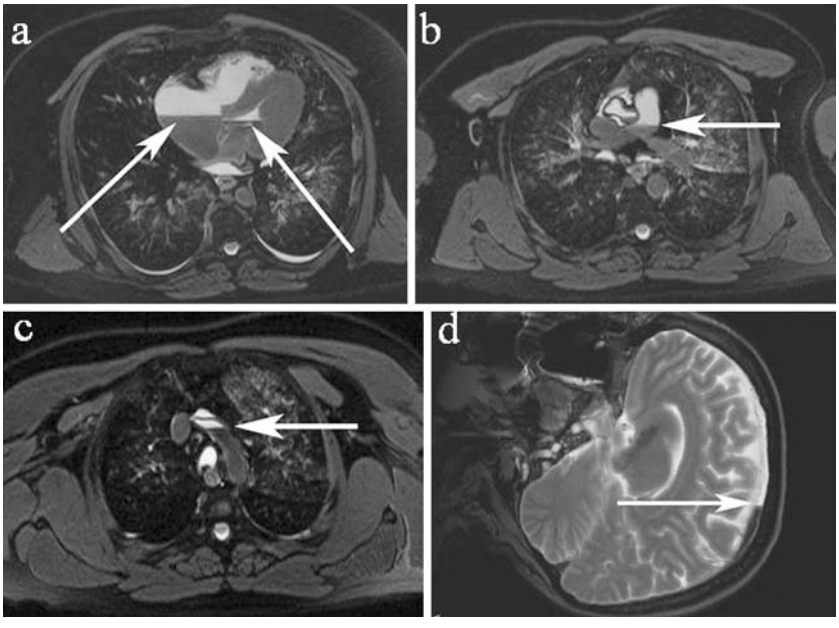

Fig. 1 **a**–**d** Sedimentation within the vascular system visualized as typical fluid levels in axial T2-weighted MR images [TE 96 ms, TR 4,000 ms]: **a** right atrium and left ventricle and **b** pulmonary artery, **c** aortic arch, and **d** in a cranial sagittal image within the superior sagittal sinus

(100%) by MRI; 35 of the cases (79.5%) showed visible internal livores within the lungs and 10 (23%) within the liver. In 14 cases (31.8%), postmortem clotting was seen and all showed postmortem clots within the right heart or pulmonary artery, but only 10 of the 44 cases showed postmortem clots within the left chambers of the heart or the aorta.

Table 1 Frequency of postmortem alterations in the 44 cases included in the Virtopsy project

IRM. Nr.	Cause of death	Liv. lungs	Liv. liver	c. rA	c. rV	c. IA	c. IV	c. pa	c. aor.
1	Gunshot to the head	+	+	−	−	−	−	−	−
2	Polytrauma	+	−	−	−	−	−	−	−
3	Polytrauma	+	+	−	−	−	−	−	−
6	Cardiac insufficiency	+	−	+	+	+	−	+	+
10	Hanging	+	−	−	−	−	−	−	−
13	Cardiac insufficiency	+	−	+	+	−	−	+	+
14	Cardiac insufficiency	+	−	−	−	−	−	−	−
15	Polytrauma	+	−	−	−	−	−	−	−
16	Gunshot to the head	+	+	+	−	+	+	−	+
17	Cardiac insufficiency	+	−	−	−	−	−	−	−
21	Gunshot to the head	+	−	+	−	−	−	−	−
23	Air embolism	+	−	−	−	−	−	−	−
24	SIDS	−	+	−	−	−	−	−	−
25	Cardiac insufficiency	−	−	−	−	−	−	−	−
26	Cardiac insufficiency	+	−	−	−	−	−	−	−
30	Bleeding	+	−	+	+	+	−	+	−
31	Gunshot to the head	+	+	−	−	−	−	−	−
34	Drowning	+	+	−	−	−	−	−	−
35	Polytrauma	+	+	−	−	−	−	−	−
36	Knife wound to the heart	+	−	−	−	−	−	−	−
37	Cardiac insufficiency	+	−	+	+	−	−	−	−
39	Drowning	+	−	−	−	−	−	−	−
40	Fracture of dens axis	+	+	−	−	−	−	−	−
43	Endocarditis	−	−	−	−	−	−	−	−
45	Cardiac insufficiency	+	−	−	−	−	−	−	−
48	Cardiac insufficiency	+	−	+	+	+	+	+	+
53	Hypothermia	+	−	+	−	+	−	−	−
63	Polytrauma	+	−	−	−	−	−	−	−
69	Polytrauma	+	−	+	+	+	−	+	−
72	Gunshot to the head	−	−	+	−	−	−	−	−
73	Gunshot to the head	−	+	−	−	−	−	−	−
74	Polytrauma	−	−	−	−	−	−	−	−
76	Drowning	+	−	−	−	−	−	−	−
77	Drowning	−	−	−	−	−	−	−	−
78	Fatal hemorrhage	+	−	+	+	−	−	+	−
81	Pneumothorax	−	−	−	−	−	−	−	−
84	Intracranial pressure	+	−	−	−	−	−	−	−
85	Cardiac insufficiency	−	−	−	−	−	−	−	−
88	Polytrauma	+	+	−	−	−	−	−	−
89	Bleeding	+	−	−	−	−	−	−	−
90	Cardiac insufficiency	+	−	+	+	+	−	+	−
91	Strangulation	+	−	−	−	−	−	−	−
92	Intoxication	+	−	+	+	+	−	+	−
93	Cardiac insufficiency	+	−	+	+	−	−	+	+

The case number and the cause of death are shown. The presence of internal livores (liv.) within the lungs and liver and postmortem clotting (c.) within right atrium (rA), right ventricle (rV), left atrium (lA), left ventricle (lV), pulmonary artery (pA), or aorta (aor.) was observed (+) or not (−)

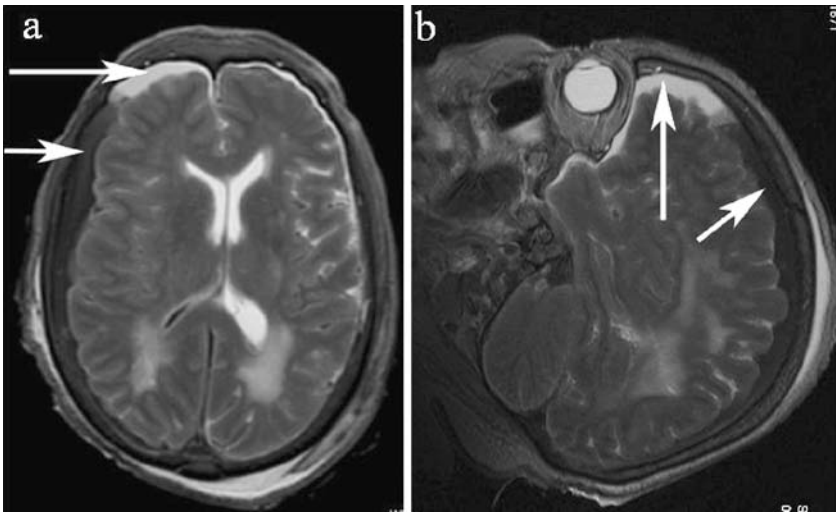

Fig. 2 **a** Subdural hematoma in postmortem axial and **b** sagittal T2-weighted MR images [TE 96 ms, TR 4,000 ms]. Sedimentation phenomena are visible in the space between dura and arachnoidea (*long* and *short arrows*). Note the dislocation of the midline toward the left side as well as left occipital and right parietal subcutaneous swelling

Sedimentation within the systemic circulatory system

The components of blood are separated by gravity, which leads to typical fluid levels in blood-filled cavities such as the major vessels and cardiac cavities (Fig. 1) [9]. Similar postmortem findings outside the vascular system were visible in pathological blood-filled cavities of the chest, the abdomen, or the subdural space and were considered to be diagnostic signs of internal bleeding in postmortem imaging (Fig. 2). Furthermore, visible sedimentation in subcutaneous or intramuscular hematomas indicated a wound cavity as often created by blunt force trauma, e.g., decollement in vehicle accidents (Fig. 3). Postmortem MRI sequences provided different contrasts of this phenomenon. At room temperature, the best contrast was visible on T2-weighted and on inversion recovery sequences (Fig. 4). Serum in the upper layer showed an intense signal, and the cellular components, predominantly erythrocytes in the lower position, were imaged with weaker signals on T2-weighted images. Often, a small layer of thrombocytes and leukocytes was also visible between the layers of serum and erythrocytes with intermediate signal intensity, depending on the status of postmortem clotting and thrombolysis. Therefore, these sequences were superior especially when minor internal bleeding was present. T1-weighted sequences reached only low contrast when the corpse was scanned at room temperature because of the temperature dependence of spin-lattice relaxation [6]. Postmortem CT has already been shown to reveal these layers within the heart [23], but postmortem MRI was able to image this phenomenon at higher contrast, more precisely, and with more details [20, 13]. Widespread postmortem clotting led to a reduction of sedimentation, as cellular components of the blood were enclosed within the clot. Sedimentation as a physiological postmortem alteration was seen in all of the cases studied.

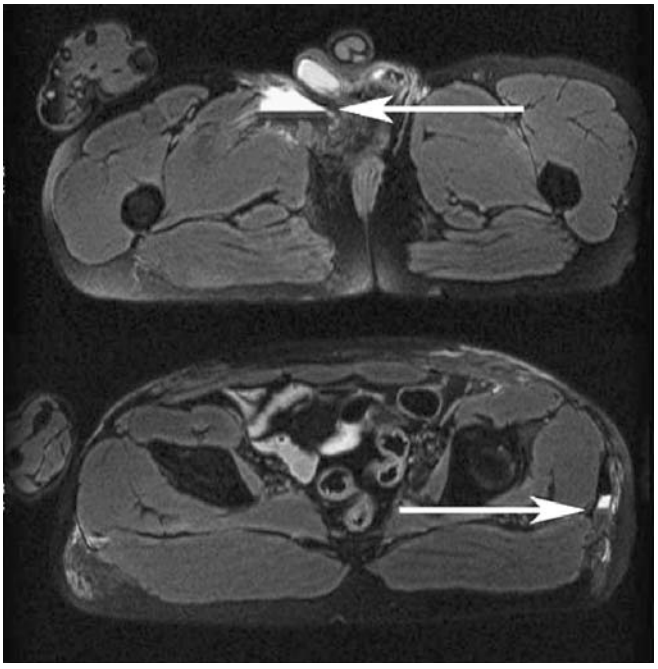

Fig. 3 Axial T2-weighted pelvic MR images (TE 96 ms, TR 4,000 ms) of blood-filled wound cavities (décollements) in a pedestrian/vehicle accident. Sedimentation and fluid levels (*arrows*) within the subcutaneous tissue are visible as a postmortem radiological hint for wound cavities

Sedimentation within the capillary system of internal organs (internal livores)

Sedimentation also occurred within the capillary system of the liver, lungs, kidneys, and well-vascularized muscles, e.g., the heart and preexisting collagenous capsules, e.g., visceral pleura or epicardium form natural borders. The small vessels in the lower regions of the organ filled by erythrocytes showed a reduction of the signal in T2-weighted images. Shortly after death, the organ showed a homogeneous organ-specific signal with a hypointense lower layer. In the absence of a cavity, the signal behavior of sedimentation within the small vessels is superimposed

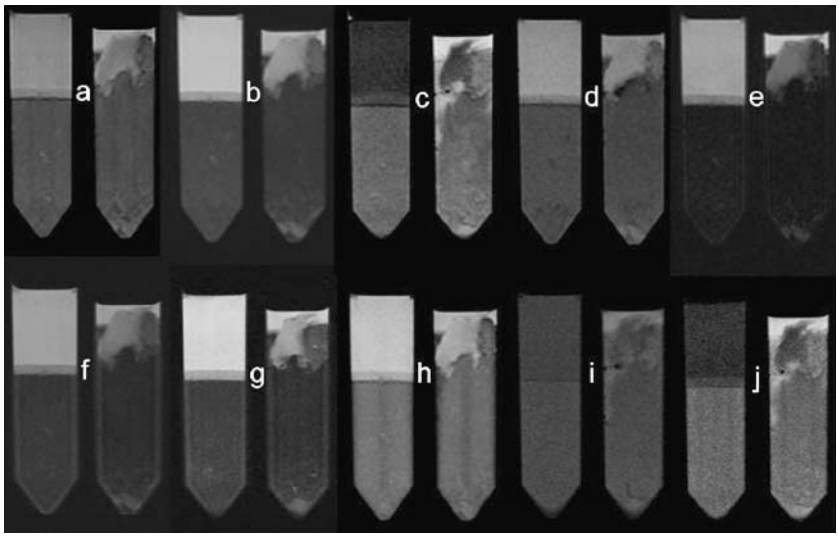

Fig. 4 **a**–**j** Sedimented blood (*left*) and blood with postmortem clotting (*right*) in ten of the most used MRI sequences in postmortem imaging showing the differences in contrast at room temperature (22°C). **a** PD-weighted (TE 15 ms, TR 4,000 ms), **b** T2-weighted (TE 90 ms, TR 4,000 ms), **c** T1-weighted (TE 14 ms, TR 400 ms), **d** gradient recalled at steady state sequence (TE 8 ms, TR 300 ms), **e** fluid-attenuated inversion recovery (TE 217.5 ms, TI 2,200 ms, TE 11,002 ms), **f** T2-weighted (TE 96 ms, TR 4,000 ms), **g** fat saturation T2-weighted (TE 105 ms, TR 4,000 ms), **h** short tau inversion recovery (TE 15 ms, TI 135 ms, TR 3,000 ms), **i** true fast imaging with steady state precession (TE 6.4 ms, TR 110 ms), **j** fat saturation T1-weighted (TE 15 ms, TR 400 ms)

on the normal signal intensity of the organ, but there was no precise fluid level visible as seen in great vessels (Fig. 5).

Differences in the histological structure of the organs caused different sedimentation characteristics as already shown for livores of the skin [8], and this correlated to different imaging appearances of internal livores in each organ.

The lungs showed sedimentation with internal livores in 35 cases (79.5%) very well in MSCT and MRI [30]. The density difference between air and blood causes the contrast of the dilated and dense-filled vessels displacing the air-filled alveoli in the lower areas and leaving more air-filled alveoli in the upper parts of the lungs (Fig. 6).

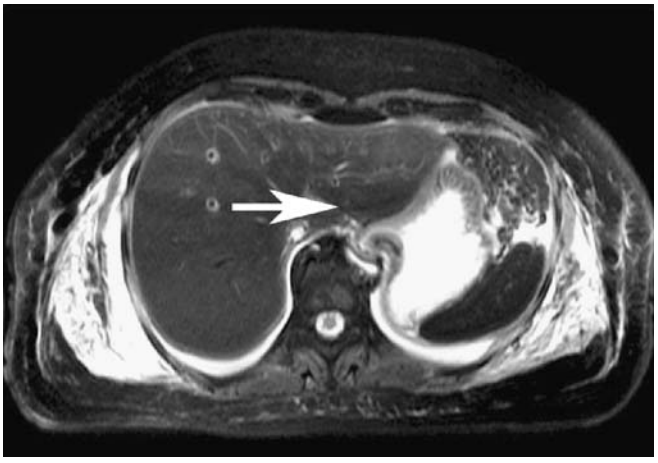

Fig. 5 Axial T2-weighted MR image (TE 96 ms, TR 4,000 ms) of internal livores within the left lobe of the liver; noticeable is a vertical loss of signal with a hypointense layer in the lower region (*arrow*)

Even ultrasonographic densitometry was able to measure the difference caused by hypostasis as already shown in the lungs [18]. The MRI appearance of internal livores in the lungs is different from other parenchymal organs and in T2-weighted sequences comparable to the appearance in MSCT. Because of the low signal intensity of the air-filled alveoli, internal livores caused a relative hyperintense signal in the lower areas of the lungs in contrast to upper parts of the same or adjacent lobes (Fig. 6). This postmortem appearance is similar to the radiological appearance of a local pneumonia and is therefore nonspecific. Comparison to livores elsewhere in the corpse should help to distinguish between these two conditions.

In the parenchyma of the liver and spleen, hypostasis was not as well visualized as within the lungs but appeared in lower regions as an indistinct hypointense layer on the T2-weighted sequences in ten cases (23%). A similar phenomenon has already been shown for the lower-situated regions of the myocardium [13]. The distinctness of the internal livores depends on the residual intravascular blood volume and the signal of the organ tissue itself. Therefore, internal livores were hardly or not even visible by imaging in cases of fatal bleeding correlating to the experience of reduced livores in the skin.

The differential diagnosis can sometimes be complicated by postmortem alterations occurring in parallel, such as putrefaction, and both have to be separated from intravital pathological findings. The putrefaction gas also reduces signal intensity in T2-weighted images but can be discerned by visualizing the gas in MSCT (Fig. 7 shows a case of putrefaction). Therefore, a putrid liver in a corpse with normal blood volume shows three levels of different signal intensities in MRI: the upper hypointense layer caused by putrefaction gas, a middle homogeneous layer of less af-

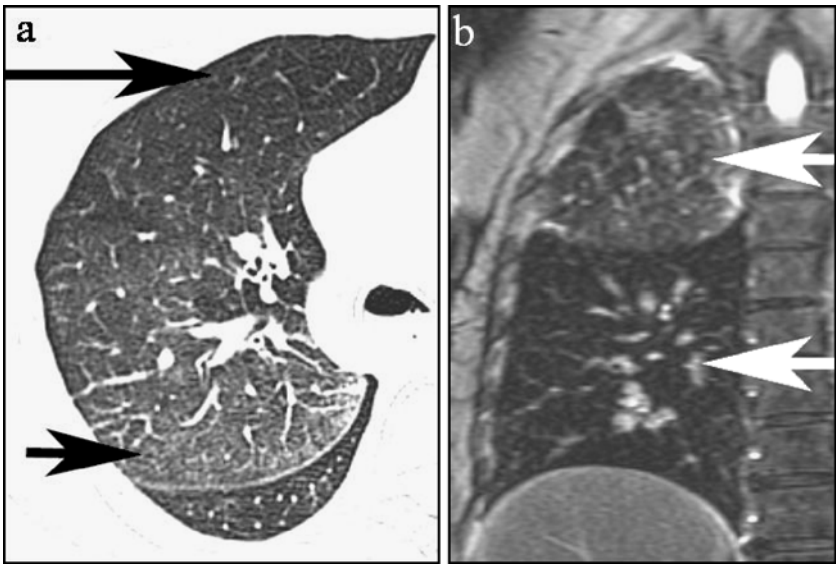

Fig. 6 **a** Internal livores in right upper pulmonary lobe in axial MSCT and **b** coronal T2-weighted MR image (TE 96 ms, TR 4,000 ms). Note the hyperdensities in the lower areas of the right upper pulmonary lobe (*small arrow*) in contrast to the hypodensities of the upper parts (*large arrow*) and to the right lower lobe below; on coronal T2-weighted MR images, internal livores appear hypointense in contrast to other parenchymal organs (*upper arrow*)

fected liver tissue, and a lower hypointense layer caused by sedimentation. In contrast to other authors [20], we prefer T2-weighted images to distinguish postmortem lividity.

Postmortem clotting

The cessation of the circulation induces clotting processes as already described for the postmortem clots within the cardiac cavities [12], because the fibrinogen within the postmortem serum as well as the platelets are still capable of functioning for a variable postmortem period. There is still no consensus in the literature, whether in cases of sudden death no clotting occurs, if postmortem clots have already been dissolved by fibrinolysis or if both reactions occur in parallel and no clotting is visible. In our opinion, the latter explanation is the most plausible, because high levels of catecholamines and low pH, as often seen in these

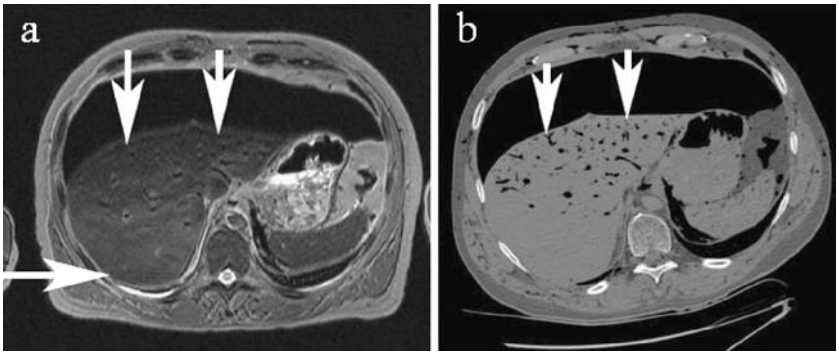

Fig. 7 **a** Internal livores of the liver at beginning putrefaction in an axial T2-weigted MR image (TE 96 ms, TR 4,000 ms); hypointense regions are visible in the upper (*short arrows*) and lower (*longer arrow*) parts of the liver. **b** Upper loss of signal is caused by putrefaction gas as seen in MSCT and the lower hypointense region corresponds to sedimented cellular components of the blood

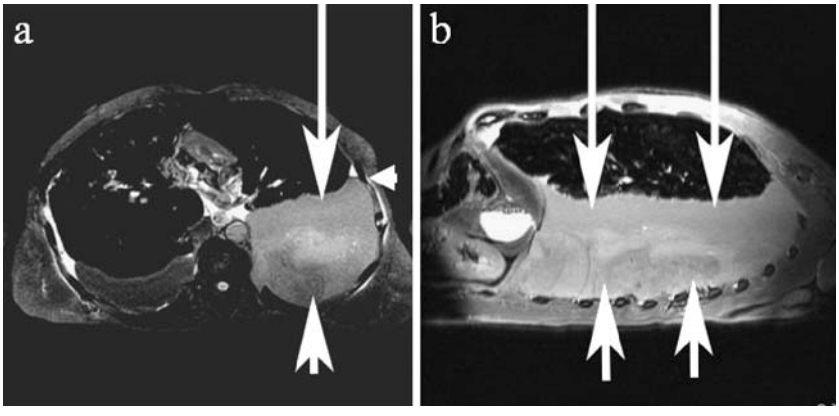

Fig. 8 **a** Axial and **b** sagittal T2-weighted thoracic MR images (TE 96 ms, TR 4,000 ms) of a fatal internal bleeding. Postmortem clotting within the hematoma after several rotations of the corpse prior to scanning shows inhomogeneous signal intensities with even vertical-fixed sedimentation levels within the clotting (*short arrows*). Within the upper layer (*longer arrows*), resedimentation begins; note small level (*arrow head*) laterally of the left lung in the axial image

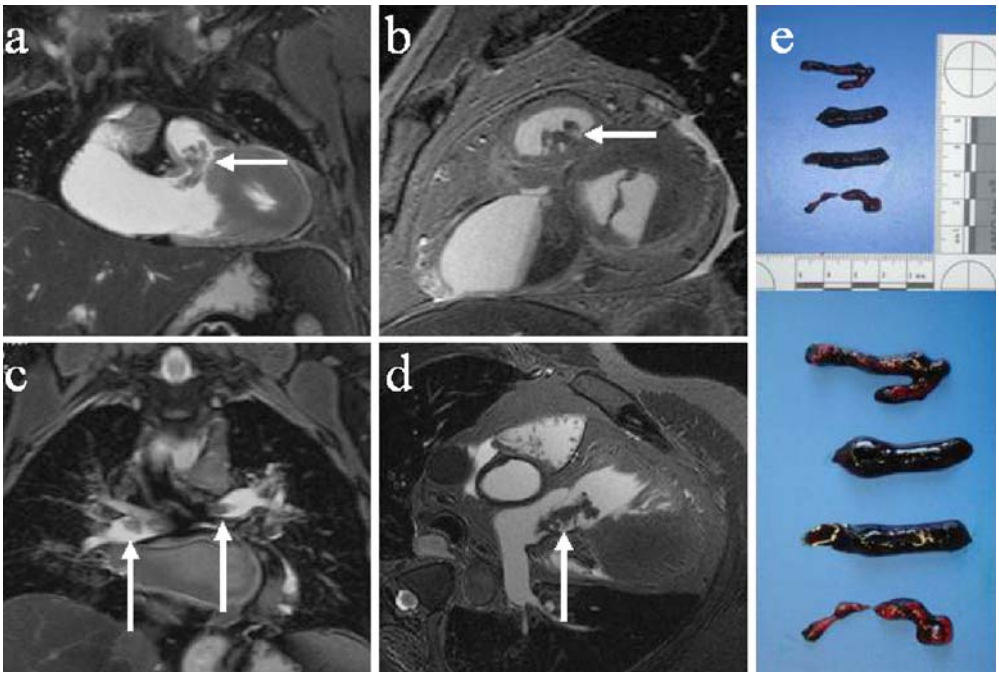

Fig. 9 **a**–**e** Postmortem clotting within **a** right ventricular outflow tract and **b** pulmonary artery trunk in T2-weighted (TE 90 ms, TR 4,000 ms) short axis images (**a** + **b**), **c** a coronal chest image and **d** a long axis image simulating an embolism of pulmonary artery. **e** Autopsy appearance of the postmortem clots that were found

cases, induce fibrinolysis by increasing the release of plasminogen activator from the vascular wall [27–29]. Supporting this explanation is the experience that clotting mostly begins within the cardiac cavities and the major vessels. The ratio between the vessel wall surface area and blood volume is lower in the great vessels and should lead to a lower local concentration of plasminogen activator. Additionally, in a case of fatal internal bleeding, we found extensive clotting within the blood that had been in the thoracic cavity (Fig. 8) but only sparse clotting of the remaining blood within the vascular system. In this case, sedimentation was less, because the corpse was found in a prone position and was turned several times prior to the final scanning position (inspection, washing). The sedimentation process of the cellular components was renewed (note the small level lateral of the left lung in Fig. 8a), and the postmortem clots retained their structure after turning the corpse and were found in the lower layer. Sedimentation and clotting processes can occur in parallel, and therefore, sedimentation fractions can be fixed within the clot and different constitutions can occur. Fast clotting and slower sedimentation enclose erythrocytes prior to separation and lead to homogeneous clots. Slower clotting and fast sedimentation (e.g., antemortem inflammation) divide the clot into a more signal-intensive, predominantly fibrin-containing upper portion and an erythrocyte-filled lower region with less signal intensity on T2-weighted images. This leads to irregular and even vertical sedimentation levels within the clots after turning the corpse (Figs. 4 and 8). This can be used to differentiate between vital or postmortem clotting. Vital clots should not show any sedimentation within the clot and are imaged as a homogeneous structure that has direct contact to the wall of the cardiac cavity or the vessel wall [2]. Hemosiderin-induced effects (loss of signal in MRI) as a sign of vital conversion of hemoglobin of enclosed erythrocytes should also not be seen [10, 11]. The distinction between vital and postmortem clots will still be a challenge for postmortem imaging, as postmortem clots can simulate all kinds of embolism (Fig. 9). Therefore, a minimal invasive biopsy technique has to be implemented to overcome this difficulty by using histological investigations of the clot specimen to support or refute the assumed diagnosis. In 14 of our cases (31.8%), postmortem clotting was seen within the cardiac cavities or the major vessels. The occurrence slightly preferred the right heart and its major vessels (Table 1). The ability to visualize postmortem clotting in imaging is a further finding that can be used as a hint for or against sudden death (cave: exclusion of anticoagulation therapy).

Table 2 displays our experience of the strengths and weaknesses of both methods. Except for the visualization of internal livores within the lungs, we consider MRI as more precise and accurate compared to MSCT in the demonstration of physiological postmortem alterations. The density difference between air and blood makes MSCT superior for the visualization of internal livores within the

Table 2 Strengths and weaknesses of MSCT and MRI in visualization of physiological postmortem alterations: ++ excellent, + sufficient, (+) minimal information, and – no visualization

Postmortem alteration	MSCT	MRI
Sedimentation	(+)	++
Int. liv. lungs	++	+
Int. liv. liver	–	+
Postmortem clotting	(+)	++

lungs. All further postmortem alterations that occur within tissue or blood are better imaged using the signal intensity differences in predominantly T2-weighted MRI sequences.

Conclusions

Knowledge about the different appearances in postmortem imaging that are caused by normal postmortem alterations of blood and its components is of utmost importance to distinguish them from pathological findings. Sedimentation, internal livores, and postmortem clotting are physiological alterations of the corpse and can be imaged during postmortem using predominantly MRI and additionally CT. Therefore, forensically relevant information about the cause of death can be radiologically obtained (internal bleeding, wound cavities, etc.). There is still a need to acquire further experience in postmortem imaging to define the entire common postmortem appearance of a human corpse.

Acknowledgements We would like to thank Elke Spielvogel, Christoph Laeser, Carolina Dobrowolska, and Verena Beutler for their excellent help during the scanning and Urs Königsdorfer and Roland Dorn for their experienced assistance at autopsy. We are also grateful to Therese Périnat for the histological preparations.

References

1. Aghayev E, Yen K, Sonnenschein M et al (2004) Virtopsy postmortem multi-slice computed tomography (MSCT) and magnetic resonance imaging (MRI) demonstrating descending tonsillar herniation: comparison to clinical studies. Neuroradiology 46:559–564
2. Barkhausen J, Hunold P, Eggebrecht H et al (2002) Detection and characterization of intracardiac thrombi on MR imaging. Am J Roentgenol 179:1539–1544
3. Berg S (1950) Das postmortale Verhalten des Blutes. Dtsch Z Gesamte Gerichtl Med 40:1–75
4. Bohm E (1987) Structural principles of hemostatic processes. Forensic Sci Int 33:7–22
5. Bohm E, Hochkirchen KH (1983) Ultrastructure of intravital, postmortem and autolysed fibrin. Forensic Sci Int 21: 117–127
6. Farahani K, Saxton RE, Yoon HC et al (1999) MRI of thermally denatured blood: methemoglobin formation and relaxation effects. Magn Reson Imaging 17:1489–1494
7. Foroughi E (1971) Serum changes in drowning. J Forensic Sci 16:269–282
8. Hellerich U, Bohnert M, Pollak S (2001) Hypostasis-induced changes in the breast area. Arch Kriminol 207:162–169
9. Huisman TA (2004) Magnetic resonance imaging: an alternative to autopsy in neonatal death? Semin Neonatol 9:347–353
10. Imaizumi T, Chiba M, Honma T et al (2003a) Detection of hemosiderin deposition by T2*-weighted MRI after subarachnoid hemorrhage. Stroke 34:1693–1698
11. Imaizumi T, Chiba M, Honma T et al (2003b) Dynamics of dotlike hemosiderin spots associated with intracerebral hemorrhage. J Neuroimaging 13:155–157
12. Jackowski C (2003) Macroscopical and histological findings in comparison with CT- and MRI- examinations of isolated autopsy-hearts. Thesis, University of Magdeburg
13. Jackowski C, Schweitzer W, Thali M et al (2005) Virtopsy: postmortem imaging of the human heart in situ using MSCT and MRI. Forensic Sci Int 149:11–23
14. Jeanmonod R, Staub C, Mermillod B (1992) The reliability of cardiac haemodilution as a diagnostic test of drowning. Forensic Sci Int 52:171–180
15. Laiho K, Penttila A (1981) Autolytic changes in blood cells and other tissue cells of human cadavers. I. Viability and ion studies. Forensic Sci Int 17:109–120
16. Noriko T (1995) Immunohistochemical studies on postmortem lividity. Forensic Sci Int 72:179–189
17. Penttila A, Laiho K (1981) Autolytic changes in blood cells of human cadavers. II. Morphological studies. Forensic Sci Int 17:121–132
18. Quan L, Zhu BL, Fujita MQ et al (2003) Ultrasonographic densitometry of the lungs at autopsy: a preliminary investigation for possible application in forensic pathology. Leg Med (Tokyo) 5(Suppl 1):S335–S337
19. Rammer L, Gerdin B (1976) Dilution of blood in fresh water drowning. Post-mortem determination of osmolarity and electrolytes in blood, cerebrospinal fluid and vitreous humor. Forensic Sci 8:229–234
20. Roberts IS, Benbow EW, Bisset R et al (2003) Accuracy of magnetic resonance imaging in determining cause of sudden death in adults: comparison with conventional autopsy. Histopathology 42:424–430
21. Sannohe S (2002) Change in the postmortem formation of hypostasis in skin preparations 100 micrometers thick. Am J Forensic Med Pathol 23:349–354
22. Schleyer F (1958) Postmortale Blutviscosität, Blutzellvolumen, osmotische Erythrocytenresistenz und Blutkörperchensenkung in Beziehung zu Leichenalter und Todesursache. Virchows Arch 331:276–286
23. Shiotani S, Kohno M, Ohashi N et al (2002) Postmortem intravascular high-density fluid level (hypostasis): CT findings. J Comput Assist Tomogr 26:892–893
24. Shiotani S, Kohno M, Ohashi N et al (2004) Non-traumatic postmortem computed tomographic (PMCT) findings of the lung. Forensic Sci Int 139:39–48
25. Skopp G, Potsch L, Lutz R et al (1998) Hemoglobin diffusion across a venous wall: an experimental study. Am J Forensic Med Pathol 19:372–376
26. Stammers AH, Vang SN, Mejak BL et al (2003) Quantification of the effect of altering hematocrit and temperature on blood viscosity. J Extra Corpor Technol 35:143–151
27. Takeichi S, Wakasugi C, Shikata I (1984) Fluidity of cadaveric blood after sudden death: part I. Postmortem fibrinolysis and plasma catecholamine level. Am J Forensic Med Pathol 5:223–227
28. Takeichi S, Wakasugi C, Shikata I (1985) Fluidity of cadaveric blood after sudden death: part II. Mechanism of release of plasminogen activator from blood vessels. Am J Forensic Med Pathol 6:25–29
29. Takeichi S, Tokunaga I, Hayakumo K et al (1986) Fluidity of cadaveric blood after sudden death: part III. Acid-base balance and fibrinolysis. Am J Forensic Med Pathol 7:35–38
30. Thali MJ, Yen K, Schweitzer W et al (2003) Virtopsy, a new imaging horizon in forensic pathology: virtual autopsy by postmortem multislice computed tomography (MSCT) and magnetic resonance imaging (MRI)—a feasibility study. J Forensic Sci 48:386–403
31. Thomsen H, Krisch B (1994) The postmortem activation status of platelets. Int J Legal Med 107:111–117
32. Thomsen H, Kaatsch HJ, Krisch B (1999) How and why does the platelet count in postmortem blood change during the early postmortem interval? Forensic Sci Int 101:185–194
33. Yen K, Sonnenschein M, Thali MJ et al (2005) Postmortem multislice computed tomography and magnetic resonance imaging of odontoid fractures, atlantoaxial distractions and ascending medullary edema. Int J Legal Med 119:129–136